

of the hydrogen atoms were calculated (C-H bond length 0.95 Å; idealized  $sp^2$  geometry), and isotropic thermal parameters were assigned.

The "position" of the phosphido phosphorus lone pair was determined by locating a dummy hydrogen atom near P(2) with the idealized geometry for a bonded tertiary hydrogen. Torsion angles involving the lone pair were calculated from this dummy atom.

**X-ray Crystal Structure of 4d.** Crystals of **4d** were obtained as indicated above, and X-ray data were collected as described for **4a**. Lattice parameters (Table II) were determined from 15 centered reflections with  $2\theta$  between  $16^\circ$  and  $29^\circ$ . The data were corrected for Lorentz and polarization effects. During data collection, the intensity of individual standard reflections decreased 18–40%. The decrease for each reflection was reasonably linear, with a correlation coefficient of 0.92–0.94 for a least-squares fit. The crystal decomposed in the beam before an absorption correction could be determined. Of 4350 unique reflections collected with  $2\theta < 50^\circ$ , 3080 with  $I > 2.5\sigma(I)$  were used in the final refinement.

The structure was solved by standard heavy-atom techniques with the UCLA Crystallographic Package.<sup>49</sup> Hydrogen atoms were generally placed in assigned positions, except on the methyl groups, where one hydrogen atom was located on the difference map and the others were assigned. Non-hydrogen atoms were refined with anisotropic thermal parameters, giving two atoms that refined to non-positive definite thermal parameters. The thermal parameters of these two atoms were made

isotropic and refined further. Anomalous dispersion corrections were applied throughout the refinement. The position of the phosphido phosphorus lone pair was calculated as described for **4a**.  $\Delta/\sigma(\max)$ : 0.016.

**MO Calculations.** Extended-Hückel MO calculations<sup>50</sup> were conducted with weighted  $H_{ij}$  formula. The rhenium and  $PH_3$  phosphorus atoms of model compound ( $\eta^5-C_5H_5$ )Re(NO)( $PPH_3$ )( $PH_2$ ) were assigned idealized octahedral and tetrahedral geometries, respectively. The Re- $PH_2$  distance was set at 2.461 Å (Re- $PAR_2$  distance in **4a**), and the  $PH_2$  phosphorus-hydrogen bond distances were set at 1.44 Å. The remaining bond lengths and  $H_{ij}$  and  $\zeta$  parameters used were the same as employed previously.<sup>16</sup> For each conformation  $\theta$ , energy was minimized by rotating the Re- $PH_3$  bond (the same rotamer was optimum for all  $\theta$ ).

**Acknowledgment.** We thank the NSF for support of this research and A. T. Patton for assistance with the X-ray structure of **4d**.

**Registry No.** **1**, 92695-37-9; (-)-(S)-**1**, 110043-17-9; **2a-TsO<sup>-</sup>**, 96213-74-0; **2b-TsO<sup>-</sup>**, 113158-32-0; (-)-(S)-**2b-TsO<sup>-</sup>**, 113036-42-3; **2c-TfO<sup>-</sup>**, 113036-35-4; **2d-TfO<sup>-</sup>**, 113036-37-6; **3**, 92695-35-7; **4a**, 96213-75-1; **4b**, 98330-68-8; (+)-(S)-**4b**, 98461-38-2; **4c**, 113036-38-7; **4d**, 113036-39-8; **5a-Cl<sup>-</sup>**, 96213-76-2; **6a**, 96213-77-3; **6d**, 113036-43-4; ( $\eta^5-C_5H_5$ )Re(NO)( $PPH_3$ )( $PH_2$ ), 113036-40-1; P(*p*-Tol)<sub>2</sub>H, 1017-60-3; PEt<sub>2</sub>H, 627-49-6; PPh<sub>2</sub>H, 829-85-6; P(*t*-Bu)<sub>2</sub>H, 819-19-2.

**Supplementary Material Available:** Tables of hydrogen atom atomic coordinates and temperature factors for **4d** (3 pages); listing of structure factors for **4d** (15 pages). Ordering information is given on any current masthead page.

(50) (a) Hoffmann, R. *J. Chem. Phys.* **1963**, *39*, 1397. (b) Hoffmann, R.; Lipscomb, W. N. *Ibid.* **1962**, *36*, 2179, 3489; **1962**, *37*, 2872.

(49) Programs employed included CARESS (R. W. Broach, Argonne National Laboratory; CARESS incorporates features of PROFILE: Blessing, R. G.; Coppend, P.; Becker, P. *J. Appl. Crystallogr.* **1972**, *7*, 488), NORMAL, EXFFT, and SEARCH (all from the MULTAN-80 package, Peter Main, Department of Physics, University of York, York, England), and ORFLS (ORNL-TM-305), ORFFE (ORNL-TM-306), and ORTEP (ORNL-TM-5138). The least-squares refinement program, ORFLS, was modified to allow refinement of the coefficients of a scale function that was a quadratic function of exposure time: Ibers, J. A. *Acta Crystallogr., Sect. B* **1969**, *25*, 1667.

## Redox-Promoted Linkage Isomerizations of Aldehydes and Ketones on Pentaammineosmium

W. Dean Harman, Mikiya Sekine, and Henry Taube\*

Contribution from the Department of Chemistry, Stanford University, Stanford, California 94305. Received September 11, 1987

**Abstract:** Upon one-electron reduction,  $[Os(NH_3)_5(\eta^1-(CH_3)_2CO)]^{3+}$  undergoes an  $\eta^1 \rightarrow \eta^2$  isomerization at a specific rate of  $6 \times 10^3 s^{-1}$ . Through the investigation of the homogeneous oxidation of  $[Os(NH_3)_5(\eta^2-(CH_3)_2CO)]^{2+}$ , a specific rate of  $1.3 s^{-1}$  for the  $\eta^2 \rightarrow \eta^1$  isomerization has also been determined. Thus,  $\eta^2$ -coordination is preferred by 5.0 kcal mol<sup>-1</sup> for acetone bound to pentaammineosmium(II). The investigation has been extended to other aldehydes and ketones in order to explore the effects of strain, conjugation, and steric hindrance in the  $\eta^2$ -bound ligand. Pentaammineosmium(II) was also found to interact with the aromatic portion of the phenones investigated. In these complexes, the metal coordinates  $\eta^2$  to the arene, interrupting its aromaticity. Upon oxidation, an intramolecular isomerization occurs in which the Os(III) species adopt an  $\eta^1$ -coordination at the carbonyl.

Recently, we reported the crystal structure of a novel pentaammineosmium(II) complex in which an acetone ligand is coordinated  $\eta^2$  to the metal center.<sup>1</sup> Upon the one-electron oxidation of  $[Os(NH_3)_5(\eta^2-(CH_3)_2CO)]^{2+}$  (**1**), a rapid linkage isomerization occurs in which the oxymetallocycle opens to yield a ketone terminally bound to osmium(III). When the resulting species  $[Os(NH_3)_5(\eta^1-(CH_3)_2CO)]^{3+}$  is reduced, the acetone ligand reverts to  $\eta^2$ -coordination. By investigation of the rates of these redox-coupled isomerizations, both by electrochemistry and by the study of the reactivity of **1** with homogeneous oxidants, we hoped to extract the driving forces and specific rates of isomerization for both di- and trivalent osmium complexes.

Although several  $\eta^2$ -bound aldehyde and ketone complexes have been reported,<sup>2</sup> most are stable only at low temperature or when

the aldehyde or ketone contains electron-withdrawing groups; in no other case have changes in bonding mode attending a redox change been reported. We felt it worthwhile to take advantage of the special opportunity offered by our system because of the

(2) (a) Countryman, R.; Penfold, B. R. *J. Chem. Soc. D* **1971**, 1598. Countryman, R.; Penfold, B. R. *J. Cryst. Mol. Struct.* **1972**, *2*, 281. (b) Berke, H.; Bankhardt, W.; Huttner, G.; Seyerl, J. V.; Zsolnai, L. *Chem. Ber.* **1981**, *114*, 2754. (c) Kropp, K.; Skibbe, V.; Erker, G.; Krüger, C. *J. Am. Chem. Soc.* **1983**, *105*, 3353. Erker, G.; Rosenfeldt, F. *Tetrahedron Lett.* **1980**, *21*, 1637. (d) Clark, G. R.; Headfold, C. E. L.; Marsden, K.; Roper, W. R. *J. Organomet. Chem.* **1982**, *231*, 335–360. (e) Gambarotta, S.; Fioriani, C.; Chiesi-Villa, A.; Guastini, C. *J. Am. Chem. Soc.* **1985**, *107*, 2985–2986. (f) Buhro, W. E.; Georgiou, S.; Fernández, J. M.; Patton, A. T.; Strouse, C. E.; Gladysz, J. A. *Organometallics* **1986**, *5*, 956. (g) Fernández, J. M.; Emerson, K.; Larson, R. H.; Gladysz, J. A. *J. Am. Chem. Soc.* **1986**, *108*, 8268. (h) Tsou, T. T.; Huffman, J. C.; Kochi, J. K. *Inorg. Chem.* **1979**, *18*, 2311–2317. (i) Wood, C. D.; Schrock, R. R. *J. Am. Chem. Soc.* **1979**, *101*, 5421.

(1) Harman, W. D.; Fairlie, D. P.; Taube, H. *J. Am. Chem. Soc.* **1986**, *108*, 8223–8227.

facile valence change and have carried the investigation further so as to explore the effects of strain, conjugation, and steric hindrance in the  $\eta^2$ -coordinated ligand.

### Experimental Section

Infrared spectra were recorded on an IBM 98 FTIR spectrometer.  $^{13}\text{C}$  and  $^1\text{H}$  NMR spectra were recorded on a Varian XL-400 spectrometer.<sup>3</sup> Electrochemical experiments were performed under argon with a PAR Model 173 potentiostat driven by a PAR Model 175 universal programmer. Cyclic voltammograms were recorded with a Pt<sup>0</sup> working electrode (1 mm<sup>2</sup>), a Pt<sup>0</sup> counter electrode, and a Ag<sup>0</sup> wire reference, which was calibrated with the ferrocene/ferrocenium couple ( $E^\circ \approx 0.55$  V; NHE) kept in situ. The peak-to-peak separation for this couple was about 60 mV for all cyclic voltammograms reported. All potentials are reported vs the normal hydrogen electrode. Cyclic voltammograms taken at fast scan rates (1.0–500 V s<sup>-1</sup>) were recorded on a Tektronix single-beam storage oscilloscope.

The measurements required for the calculation of the equilibrium constant and the specific rate of  $\eta^2 \rightarrow \eta^1$  isomerization,  $k_b$ , for **1** were performed by a modified rotated-disk technique in which the electrode was stationary and the solution was rapidly stirred. Voltammograms were recorded with a 1800- $\mu\text{F}$  capacitor as a low-pass filter and a scan rate of 5 mV s<sup>-1</sup>. Rate measurements were performed at a fixed potential, recording the current as a function of time.

**Reagents.**  $[\text{Os}(\text{NH}_3)_5(\text{TFMS})](\text{TFMS})_2$  (TFMS =  $\text{CF}_3\text{SO}_2^-$ ) was synthesized as described by Lay et al.<sup>4</sup> Acetone was purified by vacuum distillation over  $\text{B}_2\text{O}_3$ ,<sup>5</sup>  $\text{Et}_2\text{O}$  and dimethoxyethane (DME), by distillation over NaK alloy, and MeOH, by distillation over  $\text{Mg}(\text{OMe})_2$  prepared in situ from  $\text{Mg}^\circ$  and  $\text{I}_2$  under argon.<sup>6</sup> *N,N*-Dimethylacetamide (DMA) was dried over BaO and then refluxed for 24 h and distilled from triphenylsilyl chloride.<sup>6</sup> The resulting material was then refluxed with  $\text{CaH}_2$  for 24 h and distilled to remove traces of HCl. 2,2-Dimethylpropiophenone (DMPP) was distilled over  $\text{P}_2\text{O}_5$ , and benzonitrile and acetonitrile were distilled from  $\text{CaH}_2$ .<sup>7</sup> NaTFMS was recrystallized from acetone and ether. Magnesium turnings were cleaned in a DME solution of iodine for 1 h followed by copious washing with DME and  $\text{Et}_2\text{O}$ . All other reagents were used as supplied. All solvents were deoxygenated by purging with argon, and reactions were carried out under argon atmosphere in a Vacuum Atmospheres Corp. glovebox.

**Preparation of  $[\text{Os}(\text{NH}_3)_5(\text{CH}_3)_2\text{CO}](\text{TFMS})_2$  (**1**).** Following the procedure previously described, **1** was prepared by reducing  $[\text{Os}(\text{NH}_3)_5(\text{TFMS})_3]$  with magnesium turnings in an acetone solution.<sup>1</sup> The product was recrystallized from acetone by vapor diffusion of  $\text{Et}_2\text{O}$ .

**Preparation of  $[\text{Os}(\text{NH}_3)_5(\text{PhCOPh})](\text{TFMS})_2$  (**2**).**  $[\text{Os}(\text{NH}_3)_5(\text{TFMS})_3]$  (100 mg) was dissolved in a cosolvent mixture of 10 mL of DME and 0.3 mL of DMA. Benzophenone (1.0 g) and 1.0 g of activated magnesium were added, and the solution was stirred for 40 min. The deep orange solution was then added to 100 mL of  $\text{CH}_2\text{Cl}_2$  and the resulting precipitate washed with  $\text{CH}_2\text{Cl}_2$  and  $\text{Et}_2\text{O}$ . The final product was dried under vacuum. These reaction conditions produce a 2:1 mixture of two structural isomers corresponding to the  $\eta^2$ -bound arene (**2a**) and  $\eta^2$ -bound ketone (**2b**) complexes, respectively. The isomers are partially characterized without separation.

$[\text{Os}(\text{NH}_3)_5(\text{PhCOPh-C,C}')](\text{TFMS})_2$  (**2a**).  $^1\text{H}$  NMR (acetone- $d_6$ ; 25 °C):  $\delta$  7.75 (2 H, d), 7.60 (1 H, t), 7.52 (2 H, t), 4.85 (3 H, b), 3.71 (12 H, b).  $^1\text{H}$  NMR (–80 °C): 7.70 (2 H, d), 7.62 (1 H, t), 7.55 (2 H, t), 7.75 (1 H, m), 7.15 (1 H, d), 6.62 (1 H, t), 5.75 (1 H, d), 5.50 (1 H, t), 4.82 (3 H, b), 3.82 (12 H, b).

$[\text{Os}(\text{NH}_3)_5(\text{PhCOPh-C,O})](\text{TFMS})_2$  (**2b**).  $^1\text{H}$  NMR (acetone- $d_6$ ; 25 °C):  $\delta$  7.98 (4 H, d), 7.33 (4 H, t), 7.25 (2 H, t), 5.95 (3 H, b), 4.12 (12 H, b).

**Preparation of  $[\text{Os}(\text{NH}_3)_5(\text{DMPP})](\text{TFMS})_2$  (**3**).**  $[\text{Os}(\text{NH}_3)_5(\text{TFMS})_3]$  (100 mg) was dissolved in a cosolvent mixture of 10 mL of DME and 0.3 mL of DMA. To this solution were added 1 mL of DMPP and 1.0 g of activated magnesium. The solution was stirred for 40 min. The resulting red solution was then added to 100 mL of  $\text{CH}_2\text{Cl}_2$  causing the precipitation of the product, which was then washed with ether and dried under vacuum.

Cyclic voltammetry (first scan; scan rate ( $v$ ) 200 mV/s; switching potential ( $E_s$ ) 1.0 V; –1.5 V (NHE); 0.5 N NaTFMS in DMA):  $E_{\text{p,a}} = 0.20$  V;  $E_{\text{p,c}} = -0.50$  V.  $^1\text{H}$  NMR (400 MHz; acetone- $d_6$ ; 55 °C):  $\delta$  6.95 (2 H, b), 6.87 (1 H, b), 6.20 (2 H, b), 4.77 (3 H, b), 3.60 (12 H, b), 1.37 (9 H, s).

**Preparation of  $[\text{Os}(\text{NH}_3)_5(\eta^2\text{-CH}_3\text{CHO})](\text{TFMS})_2$  (**4**).**  $[\text{Os}(\text{NH}_3)_5(\text{TFMS})_3]$  (300 mg) was dissolved in a cosolvent mixture of 10 mL of DME and 0.5 mL of DMA. Acetaldehyde (1.0 mL) and 2 g of activated magnesium were added, and the solution was rapidly stirred. After 2 h, a yellow precipitate formed, which was collected and washed with ether. The filtrate was treated with  $\text{CH}_2\text{Cl}_2$  (100 mL) to induce precipitation of the remaining fraction of product.

$^1\text{H}$  NMR (25 °C, acetone- $d_6$ ):  $\delta$  5.49 (3 H, b), 5.41 (1 H, q), 3.95 (12 H, b), 1.66 (3 H, d). IR (KBr): 3214, 3313, 1648, 1327, 842 cm<sup>-1</sup>. IR (ammines): 1267, 1162, 1030, 626 cm<sup>-1</sup>. IR (TFMS<sup>-</sup>): 2940, 2893, 2841, 1460, 1406, 1074, 896 cm<sup>-1</sup>. Anal. Calcd for  $\text{C}_4\text{H}_{19}\text{OsS}_2\text{F}_6\text{O}_7\text{N}_5 \cdot \frac{1}{2}\text{C}_4\text{H}_{10}\text{O}_2$ : C, 12.28; H, 3.83; N, 10.23. Found: C, 12.25; H, 3.99; N, 10.28.

**General Preparation of  $[\text{Os}(\text{NH}_3)_5(\text{RCN})](\text{TFMS})_3$ .** In a typical preparation, 200 mg of  $[\text{Os}(\text{NH}_3)_5(\text{TFMS})_3]$  was dissolved in 20 mL of either propylene carbonate or acetone. An excess of the desired nitrile was added (1 g), and the solution stirred for a period ranging from several hours (e.g. acetonitrile) to several days (e.g. perfluorobenzonitrile). The solution was filtered and then treated with excess ether. The resulting precipitate was filtered, washed with ether, and recrystallized from an acetone solution by vapor diffusion of ether. The yield was often quantitative.

**General Preparation of  $[\text{Os}(\text{NH}_3)_5(\text{RCN})](\text{TFMS})_2$ .** In a typical preparation, 200 mg of the Os(III)-nitrile complex was dissolved in 10 mL of acetone, and to this solution was added 1 g of Mg<sup>0</sup> turnings. The solution was stirred for 1.5 h, and then  $\text{Et}_2\text{O}$  was slowly added (50 mL) to precipitate the final product. This reduction was monitored electrochemically, and yields were quantitative.

### Results and Discussion

**$[\text{Os}(\text{NH}_3)_5(\text{CH}_3)_2\text{CO}]^{2+}$  as a Model Study.** When  $[\text{Os}(\text{NH}_3)_5(\text{TFMS})_3]$  is reduced in an acetone solution, the resulting complex  $[\text{Os}(\text{NH}_3)_5(\text{CH}_3)_2\text{CO}]^{2+}$ , in contrast to its labile ruthenium analogue,<sup>8</sup> is substitution inert. Even in the presence of  $\pi$ -acids such as acetonitrile or isonicotinamide, substitution of the acetone ligand in **1** is at least 6 orders of magnitude slower than for ruthenium.<sup>9</sup> As we have recently reported, the acetone ligand in **1** is bound  $\eta^2$  to osmium, with the M–C and M–O bond lengths being almost equivalent (2.13 (1) and 2.06 (1) Å, respectively). The carbonyl lies in a common plane, with the metal atom and three of the amines constituting a pentagonal-bipyramidal geometry. The C–O bond length has been increased from its uncoordinated value of 1.22 to 1.32 (1) Å, and the organic ligand greatly deviates from planarity as is the case with many unsaturated ligands that are  $\pi$ -bound.<sup>10</sup>

**Decrease in C–O Bond Order.** The distortion of the  $\pi$ -bound acetone ligand described above can be ascribed to a significant donation of electron density from the high-energy 5d orbitals of osmium into the ligand antibonding orbital. In addition to the structural data, both spectroscopic and chemical evidence support this conclusion. Through  $^{18}\text{O}$  labeling, an infrared absorption at 1330 cm<sup>-1</sup> has been assigned to the C–O stretching vibration in **1**. In previous studies<sup>2d,e,i</sup> of  $\eta^2$ -bound aldehydes and ketones, absorptions in the range of 1000–1200 cm<sup>-1</sup> have been reported. This large decrease from the free ligand stretching frequency (1715 cm<sup>-1</sup>) has been attributed to a significant loss in the carbonyl bond order. The  $^{13}\text{C}$  NMR of the acetone complex in  $\text{D}_2\text{O}$  shows the carbonyl and methyl carbons of the coordinated acetone to be shifted considerably upfield relative to free acetone. In particular, the carbonyl resonance has shifted from 215 to 83.5 ppm, whereas  $\eta^1$ -carbonyls, which are bonded to a metal through an oxygen lone pair, exhibit  $^{13}\text{C}$  shifts within 20 ppm of their uncoordinated value.<sup>11</sup> The carbonyl shift for  $[\text{Os}(\text{NH}_3)_5(\eta^2\text{-acetone})]^{2+}$  is consistent with those reported for other  $\eta^2$ -ketones<sup>2c,f,g,i</sup> and suggests the loss of sp<sup>2</sup> hybridization. Tolman<sup>12</sup> has shown that in  $\eta^2$ -bound olefins there is a direct correlation between the upfield shift of

(8) Baumann, J. A.; Meyer, T. J. *Inorg. Chem.* **1980**, *19*, 345–350.

(9) As measured in neat acetonitrile: the complex  $[\text{Ru}(\text{NH}_3)_5((\text{CH}_3)_2\text{CO})]^{2+}$  has been observed to undergo substitution in acetonitrile with a half-life of less than 1 s.

(10) Ittel, S. D.; Ibers, J. A. *Adv. Organomet. Chem.* **1976**, *14*, 33.

(11) Brown, J. M.; Chaloner, P. A. *J. Chem. Soc., Perkin Trans. 2* **1982**, 711–719.

(12) Tolman, C. A.; English, A. D.; Manzer, L. E. *Inorg. Chem.* **1975**, *14*, 2353.

(3) All spectra are presented (ppm) from tetramethylsilane.

(4) Lay, P.; Magnuson, R.; Sen, J.; Taube, H. *J. Am. Chem. Soc.* **1982**, *104*, 7658.

(5) Burfield, D. R.; Smithers, R. H. *J. Org. Chem.* **1978**, *43*, 3966.

(6) Perrin, D. D.; Armarego, W. L. F.; Perrin, D. R. *Purification of Laboratory Chemicals*; Oxford: New York, 1980.

(7) Solvents were distilled after 24-h reflux over  $\text{CaH}_2$ .

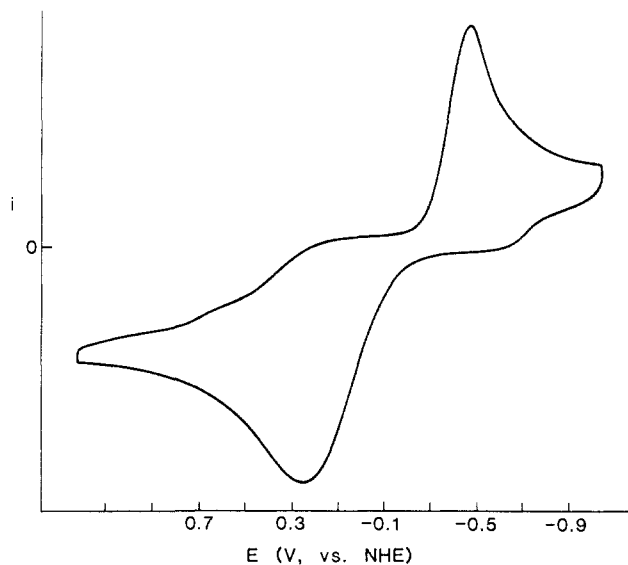


Figure 1. Cyclic voltammogram of  $[\text{Os}(\text{NH}_3)_5((\text{CH}_3)_2\text{CO})]^{2+}$ .

the olefinic carbon upon coordination and the degree of  $\pi$ -back-bonding.

**$\alpha$ -Hydrogen Exchange.** Much of the reactivity of aldehydes and ketones arises from the acidity of the  $\alpha$ -hydrogens.<sup>13</sup> This enhanced acidity, relative to hydrocarbons, is ascribed to the stability of the resulting enolate anion. In acetone the  $\text{p}K_a$  of the  $\alpha$ -hydrogen is estimated to be about 20. When acetone is terminally bound to a cationic metal center, this acidity is expected to be further enhanced by the metal stabilizing the negatively charged enolate.

An experiment was performed in which approximately equal amounts of  $[\text{Os}(\text{NH}_3)_5(\text{CH}_3)_2\text{CO}]^{2+}$  and free acetone were dissolved in a methanol- $d_4$  solution, which contained a trace of NaOMe. In contrast to terminally bound ketone complexes,<sup>14,15</sup> the exchange of the bound acetone  $\alpha$ -protons was found to be slower than that for the free ligand by a factor of at least  $10^3$ .<sup>16</sup> This remarkable contrast again can be ascribed to the reduced double-bond character of the  $\eta^2$ -bound ketone. It may be useful to draw an analogy between the present complex and an amide. In the latter, the nitrogen donates electron density into the carbonyl group, reducing the C=O double-bond character. This results in a destabilization of an enolate-like anion relative to a ketone, and thus, the acidity of the amide  $\alpha$ -protons is much lower<sup>13</sup> (*N,N*-dimethylacetamide is approximately 10 orders of magnitude less acidic than acetone). In a similar manner osmium(II) donates electron density into the carbonyl group of the ketone, resulting in a destabilization of a hypothetical  $\pi$ -bound enolate anion. On the basis of the relative proton exchange rates above, the acidity of the  $\eta^2$ -acetone ligand is expected to be several orders of magnitude lower than that of the free ketone.

**Pyrolysis.** Although **1** remains virtually unchanged after being heated under vacuum at 100 °C and over a period of 24 h, a sample heated at 150 °C under similar conditions for h decomposes,<sup>1</sup> forming a material that displays a weak infrared absorption at 1891  $\text{cm}^{-1}$ . Pentaammineosmium(II) complexes of acetaldehyde,  $\text{CO}_2$ , and DMF readily decarbonylate to give the complex  $[\text{Os}(\text{NH}_3)_5\text{CO}]^{2+}$ , which has a characteristic infrared absorption at 1899  $\text{cm}^{-1}$ .<sup>17</sup> To determine whether this is the case

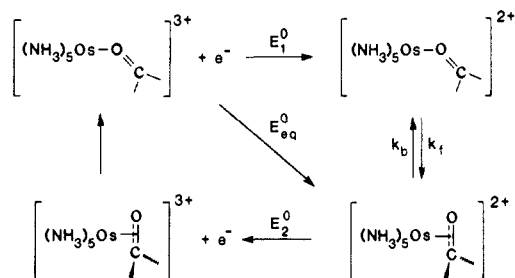


Figure 2. Schematic of redox-coupled linkage isomerizations for  $[\text{Os}(\text{NH}_3)_5((\text{CH}_3)_2\text{CO})]^{2+}$ .

for acetone as well, the thermal decomposition of **1** was investigated with a direct-insertion-probe mass spectrometer to analyze the volatile pyrolysis products. In this experiment a sample of  $[\text{Os}(\text{NH}_3)_5(\eta^2\text{-}(\text{CH}_3)_2\text{CO})](\text{TFMS})_2$  was heated under vacuum at a rate of 20 °C/min to a final temperature of 350 °C. Between 200 and 250 °C there was a sudden rise in ionization current, and the corresponding mass spectrum contained peaks at  $m/e$  43 (61%), 58 (18.3%), 42 (4.6%), and 27.1 (4.1%). These are consistent with the fragmentation pattern reported for acetone.<sup>18</sup> When the experiment was repeated with the acetone- $d_6$  analogues, a mass spectrum was obtained that contained peaks at  $m/e$  46 (100%), 45 (32%), 64 (17%), 44 (21.9%), and 30.1 (8.7%). Again, the fragmentation pattern is consistent with the expulsion of the intact acetone ligand. In neither case was there evidence for the formation of the expected product ethane.

**Electrochemistry of  $[\text{Os}(\text{NH}_3)_5(\text{CH}_3)_2\text{CO}]^{2+}$ .** A cyclic voltammogram of **1** (Figure 1) recorded in an acetone solution at 100  $\text{mV s}^{-1}$  reveals a broad, irreversible oxidation wave at +0.30 V. Both the position and breadth of the peak are scan rate dependent, the former shifting toward positive potentials as the scan rate is increased. On return, a single irreversible reduction wave at -0.45 V (NHE) appears that is not present prior to the anodic scan. When  $[\text{Os}(\text{NH}_3)_5(\text{TFMS})](\text{TFMS})_2$  is allowed to stand in a solution of dry acetone for 4 h, a cyclic voltammogram of the resulting reaction mixture shows a irreversible reduction wave at -0.45 V, which we assign the reduction of the ( $\eta^1$ -acetone)-pentaammineosmium(III) cation. The above data indicate that upon oxidation **1** undergoes a rapid linkage isomerization from  $\eta^2$  to  $\eta^1$  on osmium(III). When the resulting complex,  $[\text{Os}(\text{NH}_3)_5(\eta^1\text{-}(\text{CH}_3)_2\text{CO})]^{3+}$ , is subsequently reduced, the terminally coordinated ketone reverts back to  $\pi$ -bound (Figure 2). The peak potential of the corresponding reduction wave shows a scan rate dependence, but its half-width remains about 60 mV, suggesting reversible electron transfer followed by a rapid irreversible chemical reaction.<sup>19</sup> Consequently, the reduction of  $[\text{Os}(\text{NH}_3)_5(\eta^1\text{-}(\text{CH}_3)_2\text{CO})]^{3+}$  can be classified as an  $\text{E}_r\text{C}_i$  reaction for scan rates of 20–200  $\text{mV s}^{-1}$ .<sup>20</sup> In contrast, the oxidation wave of the  $\eta^2$ -acetone complex shows behavior consistent with quasi-reversible electron transfer over this same range of scan rates. At faster scan rates ( $v \geq 500 \text{ V s}^{-1}$ ), electron transfer becomes completely irreversible for both  $\eta^1$ - and  $\eta^2$ -isomers.

**$[\text{Os}(\text{NH}_3)_5(\text{CH}_3)_2\text{CO}]^{2+}$  as a Homogeneous Reducing Agent.** In spite of what the above electrochemical results might suggest, we found that **1** is capable of acting as a reasonably strong homogeneous reducing agent. When an acetone solution of this complex is added to 0.5 equiv of  $[\text{Os}(\text{NH}_3)_5(\text{PhCN})]^{3+}$  (PhCN = benzonitrile), the solution immediately turns deep red, indicating the rapid formation of  $[\text{Os}(\text{NH}_3)_5(\text{PhCN})]^{2+}$ , even though the reduction potential of the benzonitrile complex ( $E_{1/2} = -0.15 \text{ V}$  in acetone) is substantially negative to that of the oxidation wave of **1**, even at low scan rates. This qualitative observation was confirmed by electrochemical experiments that showed the re-

(13) Streitwieser, A.; Heathcock, C. H. *Introduction to Organic Chemistry*; Macmillan: New York, 1976.

(14) DiVaira, M.; Stoppioni, P.; Mani, F. *J. Organomet. Chem.* **1983**, *247*, 95.

(15) Michman, M.; Nossbaum, S. *J. Organomet. Chem.* **1981**, *205*, 111.

(16) NMR spectra were recorded over a 3-day period. The concentration of base is assumed to remain constant.

(17) Original references: Allen, A. D.; Stevens, J. R. *Can. J. Chem.* **1967**, *45*, 1337; **1972**, *50*, 3093.  $[\text{Os}(\text{NH}_3)_5(\text{CO})](\text{TFMS})_2$  was later prepared through the reduction of  $\text{Os}(\text{NH}_3)_5(\text{TFMS})_3$  in DMF.<sup>26</sup> NMR and IR spectra were recorded in acetone and KBr, respectively. Cyclic voltammograms were recorded in acetonitrile.

(18) *Eight Peak Index of Mass Spectra*; Unwin Brothers Ltd.: Old Woking, Surrey, U.K., 1983; Vol. 1, p 5.

(19) Bard, A. J.; Faulkner, L. R. *Electrochemical Methods Fundamentals and Applications*; Wiley: New York, 1980; pp 222 and 452.

(20) Over this range,  $E_p$  shifts negative about 30 mV per 10-fold increase in scan rate, consistent with an  $\text{E}_r\text{C}_i$  reaction.<sup>19</sup>

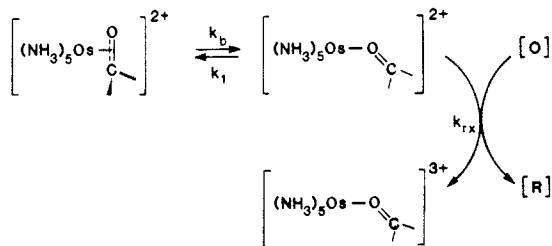


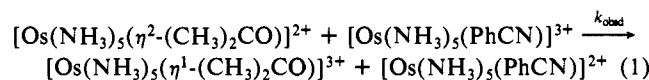
Figure 3. Homogeneous oxidation of  $[\text{Os}(\text{NH}_3)_5((\text{CH}_3)_2\text{CO})]^{2+}$ .

Table I. Kinetic Data for the Oxidation of  $[\text{Os}(\text{NH}_3)_5((\text{CH}_3)_2\text{CO})]^{2+}$  (1)

[1], <sup>a</sup> mM	[O], <sup>a</sup> mM	oxidant <sup>b</sup>	$E^\circ$ , <sup>c</sup> V	$k_f$ , <sup>d</sup> s <sup>-1</sup>
0.9	0.9	$[\text{Os}(\text{NH}_3)_5(\text{PhCN})]^{2+}$	-0.15	$1.4 \pm 0.4$
0.9	5.9	$[\text{Os}(\text{NH}_3)_5(\text{PhCN})]^{2+}$	-0.15	$1.0 \pm 0.4$
0.9	2.0	$[\text{Os}(\text{NH}_3)_5(\text{FBN})]^{2+e}$	0.09	$1.6 \pm 0.4$

<sup>a</sup> Concentration reported  $\pm 15\%$ . <sup>b</sup> Used as a TFM<sup>-</sup> salt. <sup>c</sup> Potential (NHE) measured in acetone  $\pm 0.01$  V vs  $\text{FeCp}_2$ . <sup>d</sup> Averaged over three trials. <sup>e</sup> FBN  $\equiv$  perfluorobenzonitrile.

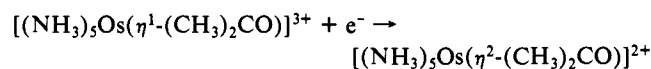
duction of the  $[\text{Os}(\text{NH}_3)_5(\text{PhCN})]^{3+}$  to be virtually complete within several seconds as shown in eq 1.



In contrast, when the identical experiment is performed with the acetonitrile analogue ( $E_{1/2} = -0.30$  V) in acetone, a measurable equilibrium is rapidly established in which approximately one-third of the Os(II) is in the form of the (acetonitrile)pentaammine complex. When the relative concentrations of the four osmium species in solution are measured, a value of 1.2 is calculated for the equilibrium constant  $K_{\text{eq}}$  where

$$K_{\text{eq}} = \frac{[\text{Os}(\text{NH}_3)_5(\text{CH}_3\text{CN})]^{2+} [\text{Os}(\text{NH}_3)_5(\eta^1\text{-(CH}_3)_2\text{CO})]^{3+}}{[\text{Os}(\text{NH}_3)_5(\text{CH}_3\text{CN})]^{3+} [\text{Os}(\text{NH}_3)_5(\eta^2\text{-(CH}_3)_2\text{CO})]^{2+}}$$

This leads to a value of  $E^\circ_{\text{eq}} = -0.30$  V (NHE) in acetone for the half-reaction



**Rate of  $\eta^2 \rightarrow \eta^1$  Isomerization of Os(II).** The reaction of 1 with  $[\text{Os}(\text{NH}_3)_5(\text{PhCN})]^{3+}$  (eq 1) can be considered a product of electron transfer and linkage isomerization. Since the anticipated oxidation potential of 1 is considerably positive to that of the oxidant, its direct oxidation followed by  $\eta^2 \rightarrow \eta^1$  isomerization seems unlikely. In a more plausible mechanism, the isomerization of acetone occurs on Os(II) *prior* to electron transfer, rendering the complex a more potent reducing agent. Provided the subsequent oxidation is fast, the overall rate of reaction for eq 1 ( $k_{\text{obsd}}$ ) should be governed by that of the  $\eta^2 \rightarrow \eta^1$  isomerization on osmium(II) (Figure 3). Furthermore, the replacement of  $[\text{Os}(\text{NH}_3)_5(\text{PhCN})]^{3+}$  in eq 1 by other oxidants should not affect this rate, provided the *direct* oxidation of  $[(\text{NH}_3)_5\text{Os}(\eta^2\text{-(CH}_3)_2\text{CO})]^{2+}$  is avoided. Thus, a series of experiments were performed in which an acetone solution of 1 was treated with an oxidant in varying concentration and potential. The rate of this reaction was monitored electrochemically, and the results are listed in Table I. In all cases, a first-order decay is observed in which the rate of oxidation deviated insignificantly over a range of potentials and concentrations. The specific rate,  $k_b$ , for  $\eta^2 \rightarrow \eta^1$  isomerization on osmium(II) is therefore assigned a value of  $1.3 \pm 0.4$  s<sup>-1</sup> in acetone.

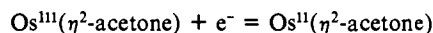
**Rate and Free Energy of  $\eta^1 \rightarrow \eta^2$  Isomerization on Os(II).** In the cyclic voltammogram of 1 over the range of scan rates 20–200 mV s<sup>-1</sup>, the reduction of  $[(\text{NH}_3)_5\text{Os}(\eta^1\text{-(CH}_3)_2\text{CO})]^{3+}$  is shown to be an electrochemically reversible reaction followed by an irreversible chemical one. In the limit of pure kinetic control,<sup>21</sup>

the peak potential of the reduction wave,  $E_p$ , will be shifted positive of the  $\eta^1$  reduction potential,  $E^\circ_1$ , as a consequence of the ensuing isomerization (eq 2). When this is coupled with a form of the  $E_p = E^\circ_1 - 0.780(RT/nF) + (RT/2nF) \ln(kRT/nFv)$  (2)

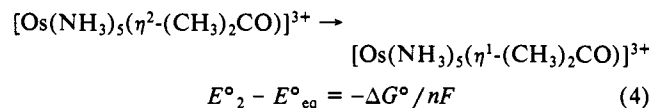
$$\Delta E = (RT/nF) \ln(k_f/k_b) \quad \Delta E \equiv E^\circ_{\text{eq}} - E^\circ_1 \quad (3)$$

Nernst equation (eq 3),  $E^\circ_1$  and  $k_f$  are determined to be  $-0.52 \pm 0.01$  V and  $(6 \pm 3) \times 10^3$  s<sup>-1</sup>, respectively, where  $k_f$  is the specific rate of  $\eta^1 \rightarrow \eta^2$  isomerization on Os(II). The reduction potential  $E^\circ_1$  is found to be similar to that measured for  $[\text{Os}(\text{NH}_3)_5(\text{CH}_3)_3\text{CCOCH}_3]^{2+}$ , a complex in which  $\eta^2$ -coordination is not observed because of steric constraints. When the specific rate of  $\eta^1 \rightarrow \eta^2$  isomerization ( $k_f$ ) is combined with  $k_b$  in eq 3, the free energy of isomerization,  $\Delta G^\circ$ , is found to be  $-5.0 \pm 0.3$  kcal/mol.

**Estimate of Isomerization Energy on Os(III).** In order to calculate the isomerization energy for acetone bound to osmium(III), the formal potential,  $E^\circ_2$ , for the half-reaction



is required. A direct measurement of this value has been unsuccessful because of the irreversible electron transfer encountered at fast scan rates. Nonetheless, a crude estimate could be made by assuming this reduction potential to be similar to that of pentaammineethyleneosmium(III), which has a reversible couple at +0.40 V in acetone.<sup>22</sup> If this value is used as an estimate for  $E^\circ_2$  and is combined with the equilibrium potential ( $E^\circ_{\text{eq}}$  in Figure 2), an approximate isomerization energy of  $\Delta G^\circ = -16$  kcal/mol for acetone on osmium(III) is calculated (eq 4).



Berke et al.<sup>23</sup> have argued that  $\pi$ -bound aldehydes are poorer  $\sigma$ -donors than olefins and support this claim with experimental data. In addition, Ittel<sup>24</sup> has found that  $\pi$ -bound aldehydes and ketones are better  $\pi$ -acids than the corresponding olefins. If these statements are valid for the present system, the true potential of the ( $\eta^2$ -acetone)pentaammineosmium(III/II) couple is expected to be positive to that of the ethylene complex, and therefore the estimated value of the free energy of  $\eta^2 \rightarrow \eta^1$  isomerization would be an upper limit.

The kinetic barrier between the  $\eta^1$  and  $\eta^2$  isomers in the Os(II)-acetone complex is quite modest. Specific rates of  $1.3 \times 10^0$  and  $6 \times 10^3$  s<sup>-1</sup> for  $k_b$  and  $k_f$  correspond to  $\Delta G^\ddagger$  values of 17.3 and 12.3 kcal/mol, respectively.<sup>25</sup> Thus, it is likely that  $\eta^1 \leftrightarrow \eta^2$  isomerizations will be facile in analogous aldehyde or ketone systems provided the energetics are not unfavorable. As an example, Fernández et al.<sup>26</sup> have recently described a series of diastereomerically pure complexes of the form  $[\text{ReCp}(\text{NO})(\text{PPh}_3)_2\text{L}]^+$  where L is an  $\eta^2$ -bound aldehyde. Coordination to Re(I) was found to activate this ligand toward stereospecific hydride reduction. A  $\pi$ -bound aldehyde is expected to experience an increase in carbonyl electron density as a result of metal back-bonding, however, and therefore should be *less* reactive toward nucleophiles, relative to the free ligand. In light of the present findings, it is reasonable to invoke an  $\eta^2 \rightarrow \eta^1$  isomerization in these Re(I)-aldehyde complexes prior to their stereospecific reduction.

**Electrochemistry as a Probe for Other Ketone Complexes.** The electrochemistry of the  $\pi$ -bound (acetone)pentaammineosmium(II) complex has been shown to differ dramatically from that of the terminally bound form. Therefore, it should be possible to determine the bonding mode of a wide variety of ketones bound to

(22) Harman, W. D. Ph.D. Thesis, Stanford University, 1987.

(23) See Reference 2b. In this case  $\sigma$ -donor refers to the capacity to donate electron density from the ligand  $\pi$ -orbital.

(24) Ittel, S. D. *J. Organomet. Chem.* **1977**, *137*, 223.

(25) Atkins, P. W. *Physical Chemistry*; Freeman: San Francisco, 1978; pp 911–913. The transmission coefficient is taken as unity.

(21) Reference 19, pp 437–442.  $kRT/nFv > 5$  as defined in this reference.

**Table II.** Cyclic Voltammetric Data of  $[\text{Os}(\text{NH}_3)_5(\text{ketone})]^{2+}$  Complexes<sup>a</sup>

ketone	$E_p(\text{anodic})$ , V	$E_p(\text{cathodic})$ , V	geometric assign <sup>t</sup>
acetone <sup>b</sup>	0.36	-0.46	$\eta^2$
cyclopentanone <sup>c</sup>	0.40	-0.57	$\eta^2$
cyclobutanone <sup>c</sup>	0.36	-0.55	$\eta^2$
$(\text{CH}_3)_2\text{CHCOCH}_3^c$	0.45	-0.45	$\eta^2$
$(\text{CH}_3)_2\text{CHCOCH}_3^c$	0.50	-0.48	$\eta^2$
$(\text{CH}_3)_3\text{CCOCH}_3^c$	-0.42	-0.48	$\eta$
$\text{PhCOC}(\text{CH}_3)_3^{c,d}$	0.25	-0.49	$\eta^2$
$\text{PhCOPh}$	0.75	-0.13	$\eta^2$

<sup>a</sup> Unless noted, all cyclic voltammograms taken at 100 mV/s in 1.0 N NaTFMS/DME solution. Values are reported  $\pm 0.03$  V vs NHE. <sup>b</sup> Recorded in acetone. <sup>c</sup> Recorded in DMA at 500 mV/s. <sup>d</sup> Ketone isomer generated electrochemically from complex 4.

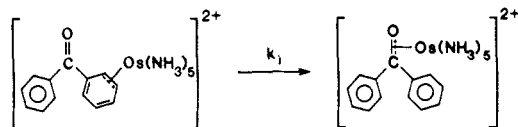
osmium(II) by comparing their electrochemical behavior with that of the parent complex.

A series of experiments was performed in which the desired (ketone)pentaammineosmium(II) complex was generated at the surface of an electrode. This was accomplished by taking a cyclic voltammogram of a solution of  $\text{Os}(\text{NH}_3)_5(\text{TFMS})_3$  in a DME solution that was 1 M in the corresponding ketone. When we scan to a potential of -1.0 V (NHE),  $[\text{Os}(\text{NH}_3)_5(\text{TFMS})]^{2+}$  is generated, which rapidly substitutes to yield the corresponding ketone-pentaammine species. A cyclic voltammogram of this complex was then taken from -1.0 to +1.0 V (NHE). The results of these experiments are shown in Table II. In all cases except for pinacolone the oxidation wave is broad and irreversible with a peak potential typically about 750 mV positive to that of the reduction wave. These results are consistent with the electrochemistry of the  $\eta^2$ -bound acetone complex discussed above and suggest that, with the exception of pinacolone, these ketones form pentaammineosmium(II) complexes featuring a  $\pi$ -bound ligand, even in cases where the carbonyl is strained or conjugated. Scan rates as high as 50 V s<sup>-1</sup> did not lead to a measurement of  $E_{1/2}$  for either the  $\eta^2$  or  $\eta^1$  isomer with any of the ketones tested.

In contrast to the electrochemical behavior of the other ketones, pinacolone shows a reversible couple at -0.45 V (NHE). The comparison of this potential with its ruthenium analogue<sup>22</sup> shows that it is in good agreement with the potential expected for a terminally bound pentaammine(ketone)osmium(III/II) species. Apparently the bulky *tert*-butyl substituent effectively blocks  $\eta^2$ -coordination. Attempts to isolate a pentaammine(pinacolone)osmium(II) species have been unsuccessful, presumably due to the lability of the  $\eta^1$ -bound ketone ligand.

**Reaction of  $[\text{Os}(\text{NH}_3)_5]^{2+}$  with Benzophenone.** When pentaammineosmium(II) is generated in the presence of benzophenone, a mixture of two isomers is formed. The NMR spectrum indicates that the minor reaction product (2b) is the anticipated  $\pi$ -bound ketone complex. The <sup>1</sup>H NMR spectrum in acetone-*d*<sub>6</sub> of this species features *cis* and *trans* ammine resonances at 4.12 (12 H) and 5.95 (3 H) ppm, respectively. Both the position and splitting of these values are consistent with the analogous acetone complex. Other resonances correspond to aromatic protons at 7.98 (d, 4 H, ortho), 7.33 (t, 4 H, meta), and 7.25 (t, 2 H, para) ppm. The ortho protons are shifted slightly downfield relative to the free ligand presumably due to the inductive effect of the complexing dipositive metal ion. Both the meta and para protons are shifted upfield, however, suggesting a general increase of  $\pi$ -electron density in the aromatic ring. These observations are consistent with those obtained for a  $\eta^2$ -bound benzophenone-Ni(0) complex characterized by Tsou et al.<sup>24</sup>

The major kinetic product of the reaction mixture (2a) features *cis*, and *trans* ammine resonances at 3.83 (b, 12 H) and 5.00 (b, 3 H) ppm and aromatic resonances at 7.75 (d, 2 H), 7.60 (t, 2 H), and 7.52 (t, 1 H) ppm. The only other feature at room temperature is an extremely broad peak in the base line of the aromatic region. Upon cooling to -90 °C, this feature splits into five peaks over the range of 5.5–7.7 ppm, each integrating to one proton. The above data indicate that the aromaticity has been interrupted in one of the rings of the benzophenone ligand.

**Figure 4.** Arene-ketone linkage isomerization with benzophenone.**Table III.** Cyclic Voltammetric Data for  $[\text{Os}(\text{NH}_3)_5(\text{DMPP})]^{2+}$ 

scan rate, mV/s	first scan		second scan	
	$E_p$ , V	$ E_{p,c} - E_{p/2} $ , mV	$E_{p,c}$ , V	$ E_{p,c} - E_{p/2} $ , mV
Cathodic Peak				
500	-0.51	60	-0.51	60
200	-0.50	60	-0.50	60
50	-0.48	60	-0.48	60
Anodic Peak				
500	0.22	62	0.25	120
200	0.20	62	0.22	90
50	0.18	60	0.18	60

<sup>a</sup> Potentials recorded  $\pm 0.01$  V vs NHE in DMA vs  $\text{FeCp}_2 \equiv 0.55$  V.

Homonuclear decoupling and chemical shift data for the ring protons are consistent with a complex in which the metal center coordinates to benzophenone in an  $\eta^2$ -fashion at the [2,3]-position of a phenyl ring (Figure 4). At room temperature, the complex apparently undergoes a tautomerization similar to that reported for  $[\text{Os}(\text{NH}_3)_5(\eta^2\text{-C}_6\text{H}_6)]^{2+}$ .<sup>26</sup>

A solution of the two isomers **2a** and **2b** was allowed to stand in acetone-*d*<sub>6</sub> for several days during which time the arene-coordinated isomer slowly converted to the ketone-bound form. An approximate half-life of 1 week has been estimated for the arene to ketone isomerization on osmium(II). After 3 days there was no significant substitution of the benzophenone ligand for the solvent.

The electrochemical behavior of **2a** is similar to that of the corresponding acetone complex. Both the oxidation wave of the  $\pi$ -bound complex and the reduction wave for the resulting pentaammine( $\eta^1$ -benzophenone)osmium(III) species are shifted to more positive potentials by about 300 mV from the respective features of the acetone analogue (Table II). This is readily explained by the conjugated aromatic rings in benzophenone, which lower the energy of the carbonyl-based  $\pi^*$ -orbital, resulting in the stabilization of the electron-rich osmium(II) metal center relative to osmium(III).

**Reaction of  $[\text{Os}(\text{NH}_3)_5]^{2+}$  with 2,2-Dimethylpropiophenone.** The properties of  $(\text{DMPP})[\text{Os}(\text{NH}_3)_5](\text{TFMS})_2$  (**3**) differ dramatically from those reported for either  $\eta^1$ - or  $\eta^2$ -bound ketones. As in the example of pinacolone, the *tert*-butyl group adjacent to the carbonyl is effective in blocking the direct formation of the  $\pi$ -bound carbonyl. Rather than forming a terminally coordinated ketone complex, the osmium is found to interact with the  $\pi$ -network of the aromatic ring. The resulting complex forms two structural isomers, resolvable by NMR at -85 °C, in which the osmium is bound  $\eta^2$  to either the [2,3]- or the [3,4]-position of the ring. Complete characterization of this and of other (arene)pentaammineosmium(II) complexes will be discussed separately.<sup>27</sup>

The electrochemical behavior of  $[\text{Os}(\text{NH}_3)_5(\text{DMPP})]^{3+/2+}$  reveals a rapid linkage isomerization upon oxidation. Cyclic voltammograms of **3** were recorded in DMA for initial and second scans at 500, 200, and 50 mV s<sup>-1</sup>. The results are listed in Table III. A cyclic voltammogram of this  $\eta^2$ -arene complex at 500 mV s<sup>-1</sup> in DMA induces a chemically irreversible oxidation wave at 0.22 V. A reverse scan results in an irreversible reduction wave at -0.51 V, a value consistent with the formation of an  $\eta^1$ -bound ketone-osmium(III) complex such as the pinacolone species described above. In contrast to the  $\eta^2$ -bound ketone complexes, the peak breadth for the oxidation wave is independent of scan rate, suggesting reversible electron transfer followed by an irreversible chemical step over this range.<sup>28</sup> When the proposed  $\eta^1$ -bound

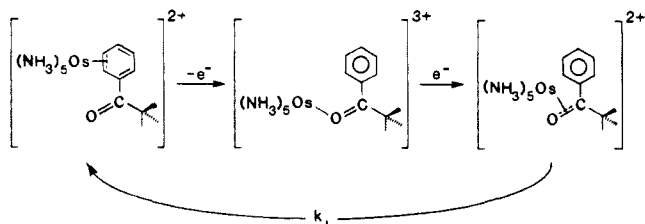
(26) Harman, W. D.; Taube, H.; *J. Am. Chem. Soc.* **1987**, *109*, 1883.

(27) Harman, W. D.; Sekine, M. S.; Taube, H., accepted for publication.

**Table IV.** Reduction Potentials for Various Pentaammineosmium(III) Species

[Os(NH <sub>3</sub> ) <sub>5</sub> (L)] <sup>2+/3+</sup> ligand (L)	E° (NHE), <sup>a</sup> V	solvent
DMA	-0.85 <sup>b</sup>	DMA
η <sup>1</sup> -(CH <sub>3</sub> ) <sub>2</sub> CO	-0.52	acetone
(CH <sub>3</sub> ) <sub>3</sub> CCOCH <sub>3</sub>	-0.45	DME
CH <sub>3</sub> CN	-0.30	acetone
PhCN	-0.15	acetone
C <sub>6</sub> F <sub>5</sub> CN	0.09	acetone
CH <sub>2</sub> CH <sub>2</sub>	0.40 <sup>b</sup>	acetone
η <sup>2</sup> -(CH <sub>3</sub> ) <sub>2</sub> CO	>0.40 <sup>c</sup>	

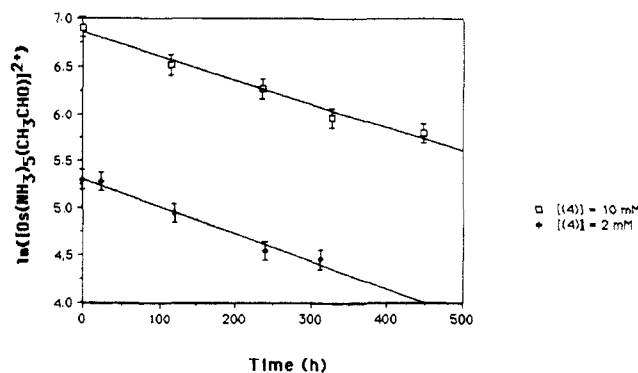
<sup>a</sup> Values reported vs NHE. <sup>b</sup> Reference 22. <sup>c</sup> Estimated value listed for comparison.

**Figure 5.** Electrochemically induced linkage isomerization with 2,2-dimethylpropiophenone.

ketone complex is reduced and the scan reversed, a new oxidation wave is formed that differs significantly from that produced by the initial scan. This second-scan oxidation wave is 30 mV positive to that observed in the initial scan and is twice as broad ( $|E_{p/2} - E_p| = 120$  mV). There appears to be no difference between the first and second reduction waves, however. The electrochemical data for all but the initial forward scan are consistent with an  $\eta^1 \rightarrow \eta^2$  ketone isomerization as outlined previously for the case of acetone. Thus, the one-electron oxidation of **3** results in an arene-to-ketone linkage isomerization in which the metal coordination site has shifted by as much as five atoms. DMA is known to react with [Os(NH<sub>3</sub>)<sub>5</sub>]<sup>3+</sup> forming an inert complex whose reduction potential (Table IV) is easily distinguished from that observed in the cyclic voltammogram of **3**. Therefore, the arene-ketone isomerization is considered to be intramolecular. When the scan rate is decreased to 50 mV/s, the second-scan oxidation wave closely resembles that of the initial scan. Apparently, this scan rate is slow enough that the  $\pi$ -bound ketone isomerizes to the more stable  $\pi$ -bound arene form prior to electrochemical oxidation. As reported for the  $\pi$ -bound acetone complex, cyclic voltammograms of [Os(NH<sub>3</sub>)<sub>5</sub>(DMPP)]<sup>2+</sup> taken at high scan rates ( $v \leq 50$  V s<sup>-1</sup>) show irreversible electron transfer. The electrochemically induced linkage isomerization of [Os(NH<sub>3</sub>)<sub>5</sub>(DMPP-C,C)]<sup>2+</sup> to [Os(NH<sub>3</sub>)<sub>5</sub>(DMPP-C,O)]<sup>2+</sup> is summarized in Figure 5.

It is significant that the preferred bonding mode for the ketone isomer of [Os(NH<sub>3</sub>)<sub>5</sub>(DMPP)]<sup>2+</sup> is  $\eta^2$ . When the phenyl group of DMPP is replaced with a methyl substituent, the corresponding pentaammineosmium(II) complex, [Os(NH<sub>3</sub>)<sub>5</sub>((CH<sub>3</sub>)<sub>3</sub>CCOCH<sub>3</sub>)]<sup>2+</sup>, is apparently terminally bound. Thus, when any steric differences are neglected, the effect of a conjugated phenyl group is to stabilize  $\eta^2$ -coordination of the ketone ligand. Presumably, the low-energy  $\pi^*$ -orbital of DMPP enhances the back-bonding interaction, which is maximized by the  $\eta^2$ -coordination.

**Reactivity of [Os(NH<sub>3</sub>)<sub>5</sub>]<sup>2+</sup> with Acetaldehyde.** Although rare,  $\pi$ -bound aldehyde complexes are more common than their ketone analogues. This has been attributed to the lower energy of the aldehyde  $\pi^*$ -orbital resulting in a more favorable back-bonding interaction with electron-rich metals. When pentaammineosmium(II) is generated in the presence of acetaldehyde, the anticipated  $\pi$ -bound acetaldehyde complex (**5**) is readily formed.

**Figure 6.** Kinetic data for the decarbonylation of [Os(NH<sub>3</sub>)<sub>5</sub>(CH<sub>3</sub>CHO)]<sup>2+</sup>.

As in the case of acetone, spectroscopic evidence shows that acetaldehyde coordinated to pentaammineosmium(II) has lost a significant amount of the carbonyl double-bond character. An infrared spectrum of the triflate salt shows no absorbances in the region of 1600–1800 cm<sup>-1</sup>, which would correspond to a typical carbonyl C–O stretch, nor does it show an absorbance in the aldehydic C–H stretch region (about 2700 cm<sup>-1</sup>). Other than TFMS<sup>-</sup> and ammine peaks, the material absorbs at 2940, 2893, 2841, 1460, 1406, and 1074 cm<sup>-1</sup>. A comparison of these with those reported for other  $\pi$ -bound aldehydes<sup>2b–g</sup> suggests an assignment of the 1074-cm<sup>-1</sup> band for the carbonyl stretch. However, both ammine and TFMS absorptions mask the region of 1300–1000 cm<sup>-1</sup>, thereby preventing conclusive assignment.

The <sup>1</sup>H and <sup>13</sup>C NMR spectra of the acetaldehyde complex are similar to those of the  $\pi$ -bound acetone complex. Cis and trans ammine proton resonances at 3.95 and 5.49 ppm are widely split, a feature common among  $\pi$ -bound complexes of pentaammineosmium(II).<sup>22</sup> The <sup>13</sup>C NMR features a carbonyl resonance at 83.4 ppm, which is dramatically shifted from the free-ligand value of about 200 ppm. As with ketones, terminally bound aldehyde complexes typically exhibit <sup>13</sup>C shifts within 20 ppm of their uncoordinated values.<sup>11</sup>

A cyclic voltammogram of **4** taken in DME (0.5 M NaTFMS, 100 mV/s) displays a broad irreversible oxidation wave at +0.42 V. The return scan reveals a broad irreversible reduction wave at -0.43 V. This behavior is consistent with that of the acetone complex and suggests an analogous redox-promoted isomerization. As in the previous cases, fast scan rates  $v \leq 100$  V/s have failed to provide additional information about the isomerization kinetics. With slower scan rates (e.g. 100 mV/s), a reversible couple is produced upon oxidation at -0.75 V in addition to the wave at -0.43 V. This is ascribed to the formation of a small amount of [Os(NH<sub>3</sub>)<sub>5</sub>(DME)]<sup>3+</sup> from the apparently labile [Os(NH<sub>3</sub>)<sub>5</sub>( $\eta^1$ -CH<sub>3</sub>CHO)]<sup>3+</sup> complex. When the cyclic voltammogram is recorded in acetonitrile, a reversible couple is produced that corresponds to [Os(NH<sub>3</sub>)<sub>5</sub>(CH<sub>3</sub>CN)]<sup>3+/2+</sup>. This is in contrast to the behavior of (acetone)pentaammineosmium(III), which shows no substitution with either DME or acetonitrile at comparable scan rates. This difference in substitution rates on osmium(III) can be understood as a manifestation of the difference in oxygen basicity between acetaldehyde and acetone.<sup>13</sup>

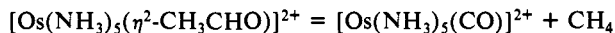
**Decarbonylation.** The synthesis of **4** described above produces about 5% of an unexpected compound (**5**), which displays a reversible couple at +1.05 V in acetonitrile. When a crystalline sample of **4** is dissolved in acetonitrile, a first-order decay is observed in which **4** decomposes to yield 1 equiv of **5**. The specific rate is determined to be  $(7 \pm 1) \times 10^{-7}$  s<sup>-1</sup> and is independent of both concentration and method of preparation (Figure 6). However, when a crude sample of **4** was dissolved in CH<sub>3</sub>CN, the specific rate of decomposition was observed to be 1 order of magnitude faster than that reported above. Thus, we believe the reported value represents the intrinsic rate of decomposition of acetaldehyde on pentaammineosmium(II), but apparently this reaction is subject to catalysis. Attempts to facilitate this reaction by the addition of trace amounts of [Os(NH<sub>3</sub>)<sub>5</sub>(CH<sub>3</sub>CHO)]<sup>3+</sup><sup>29</sup>

(28) The peak potential  $E_p$  shows the proper scan rate dependence for an E<sub>c</sub>I<sub>c</sub> mechanism analogous to that discussed in ref 19–21.



or acetaldehyde failed to alter significantly the rate of decomposition.

The product (5) displays a reversible couple at 1.02 V, a single broad NMR resonance at 3.95 ppm, and an IR stretch at 1899  $\text{cm}^{-1}$ .  $[\text{Os}(\text{NH}_3)_5(\text{CO})]^{2+}$  has been previously characterized,<sup>17</sup> and the electrochemical, NMR, and infrared data are in excellent agreement with those obtained for 5. Methane is thought to be the other major product.



In an attempt to verify this, the thermal decomposition of the aldehyde complex was investigated with a direct-insertion mass spectrometer to analyze the volatile pyrolysis products. In this experiment a sample of  $[\text{Os}(\text{NH}_3)_5(\eta^2\text{-CH}_3\text{CHO})](\text{TFMS})_2$  was heated under vacuum at a rate of 20 °C/min to a final temperature of 350 °C.

Between 180 and 200 °C there was a sudden rise in ionization current, and the corresponding mass spectrum contained peaks at  $m/e$  16 (100%), 17 (97%), 18 (39%), and 15 (37%). These are consistent with the fragmentation pattern for methane.<sup>30</sup>

**Reactivity with Formaldehyde.** Recently, a great deal of attention has been given to  $\pi$ -bound formaldehyde complexes because of their suspected role as intermediates in a homogeneous Fisher-Tropsch cycle.<sup>2b,c</sup> More generally, the fixation of formaldehyde to a metal center is considered to be a primary goal in generating metal-promoted transformations of a  $\text{C}_1$  molecule.<sup>2e</sup> When a DME solution of  $[\text{Os}(\text{NH}_3)_5(\text{TMB})]^{2+}$  (TMB = 1,2,3,4-tetramethylbenzene), a synthetic precursor to  $[\text{Os}(\text{NH}_3)_5(\text{L})]^{2+}$ ,<sup>31</sup> is treated with a dilute gas stream of  $\text{CH}_2\text{O}$ , an immediate color change to deep red occurs, but NMR and cyclic voltammetry give no indication of either an  $\eta^2$ -bound formaldehyde complex or  $[\text{Os}(\text{NH}_3)_5(\text{CO})]^{2+}$ . This reaction is currently under investigation.

(29) Generated in situ by the addition of  $[\text{FeCp}_2]\text{PF}_6$ .

(30) See reference 18, p 1.

(31) Harman, W. D.; Taube, H. *Inorg. Chem.* 1987, 26, 2917.

## Conclusion

Although  $\eta^2$ -bound aldehyde and ketone complexes are uncommon, we have found that these complexes are quite stable with pentaammineosmium(II), a strongly  $\pi$ -basic metal center. Placing bulky substituents on the ketone destabilizes the  $\eta^2$ -isomer, whereas conjugated ketones are found to stabilize this bonding mode. Although the oxidation potentials for these species are quite positive, an  $\eta^2 \rightarrow \eta^1$  isomerization renders them potent reducing agents. The utilization of the facile one-electron oxidation of these complexes has led to a determination of their specific rates and free energies of isomerization.

Pentaammineosmium(II) was also found to interact with the aromatic portion of the phenones investigated. In these complexes, the metal coordinates  $\eta^2$  to the arene interrupting its aromaticity. In the case of benzophenone, this complex eventually isomerizes to the thermodynamically favored  $\eta^2$ -ketone isomer.

A combination of the high affinity for  $\pi$ -acid ligands, kinetic stability associated with latter transition-metal complexes, and an easily accessible oxidation state make pentaammineosmium(II) ideally suited for the study of  $\pi$ -complexation and back-bonding.

**Acknowledgment.** Support of this work by National Science Foundation Grants CHE85-11658 and CHE84-14329 (400-MHz NMR) and National Institutes of Health Grant GM13638-20 is gratefully acknowledged.

**Registry No.** 1, 105164-48-5; 2a, 113161-71-0; 2b, 113161-73-2; 3, 113161-67-4; 4, 113161-69-6;  $[\text{Os}(\text{NH}_3)_5(\text{TFMS})](\text{TFMS})_2$ , 83781-30-0;  $[\text{Os}(\text{NH}_3)_5(\text{FBN})](\text{TFMS})_2$ , 113161-76-5;  $[\text{Os}(\text{NH}_3)_5(\eta^2\text{-CH}_3\text{COCH}_3)]^{2+}$ , 105164-47-4;  $[\text{Os}(\text{NH}_3)_5(\eta^2\text{-cyclopentanone})]^{2+}$ , 113161-77-6;  $[\text{Os}(\text{NH}_3)_5(\eta^2\text{-cyclobutanone})]^{2+}$ , 113161-78-7;  $[\text{Os}(\text{NH}_3)_5(\eta^2\text{-CH}_3\text{CH}_2\text{COCH}_3)]^{2+}$ , 113161-79-8;  $[\text{Os}(\text{NH}_3)_5(\eta^2\text{-}(\text{CH}_3)_2\text{CHCOCH}_3)]^{2+}$ , 113161-80-1;  $[\text{Os}(\text{NH}_3)_5(\eta^1\text{-}(\text{CH}_3)_2\text{CCOCH}_3)]^{2+}$ , 113161-81-2;  $[\text{Os}(\text{NH}_3)_5(\eta^2\text{-PhCOC}(\text{CH}_3)_3)]^{2+}$ , 113161-66-3;  $[\text{Os}(\text{NH}_3)_5(\eta^2\text{-PhCOPh})]^{2+}$ , 113161-72-1;  $[\text{Os}(\text{NH}_3)_5(\text{DMA})]^{3+}$ , 113161-82-3;  $[\text{Os}(\text{NH}_3)_5(\text{CH}_3\text{CN})]^{3+}$ , 83781-32-2;  $[\text{Os}(\text{NH}_3)_5(\text{CH}_2\text{CH}_2)]^{3+}$ , 113161-83-4; DMPP, 938-16-9;  $[\text{Os}(\text{NH}_3)_5(\text{PhCN})](\text{TFMS})_2$ , 113161-74-3; benzophenone, 119-61-9; acetaldehyde, 75-07-0; formaldehyde, 50-00-0.

## Rubidium X-ray Absorption (EXAFS and XANES) Studies of $\text{Rb}^-$ and Complexed $\text{Rb}^+$ in Alkalides and Electrides

Odette Fussa-Rydel,<sup>†</sup> James L. Dye,\*<sup>†</sup> and Boon K. Teo<sup>‡§</sup>

Contribution from the Department of Chemistry, Michigan State University, East Lansing, Michigan 48824, and AT&T Bell Laboratories, Murray Hill, New Jersey 07971.  
Received July 24, 1986

**Abstract:** The Rb K-edge X-ray absorption near-edge structure (XANES) and extended X-ray absorption fine structure (EXAFS) spectra of compounds with stoichiometries  $\text{RbNa}(18\text{C}6)$ ,  $\text{Rb}(18\text{C}6)$ ,  $\text{Rb}_2(18\text{C}6)$ ,  $\text{RbNa}(15\text{C}5)_2$ ,  $\text{Rb}(15\text{C}5)_2$ ,  $\text{Rb}(15\text{C}5)$ ,  $\text{RbK}(18\text{C}6)$ ,  $\text{CsRb}(18\text{C}6)_2$ ,  $\text{RbK}(18\text{C}6)$ ,  $\text{RbK}(15\text{C}5)_2$ ,  $\text{CsRb}(15\text{C}5)_2$ ,  $\text{Rb}(15\text{C}5)_2$ , and  $\text{Rb}_2(15\text{C}5)_2$  have been measured and interpreted. The XANES spectra provide a means of identifying the oxidation state of the rubidium-containing species in these salts. The compounds  $\text{Cs}^+(18\text{C}6)_2\text{Rb}^-$ ,  $\text{K}^+(15\text{C}5)_2\text{Rb}^-$ , and  $\text{Cs}^+(15\text{C}5)_2\text{Rb}^-$  are pure rubidides. They show no detectable EXAFS, consistent with the large size of  $\text{Rb}^-$ . The spectra of  $\text{Rb}^+(18\text{C}6)\text{Na}^-$ ,  $\text{Rb}^+(15\text{C}5)_2\text{Na}^-$ ,  $\text{Rb}^+(15\text{C}5)_2\text{e}^-$ , and  $\text{Rb}^+(15\text{C}5)_2\text{e}^-$  are similar to (but not identical with) those of the model compounds  $\text{Rb}^+(18\text{C}6)\text{Br}^- \cdot 2\text{H}_2\text{O}$  and  $\text{Rb}^+(18\text{C}6)\text{SCN}^-$ . The compounds  $\text{Rb}^+(15\text{C}5)_2\text{Rb}^-$ ,  $\text{Rb}^+(18\text{C}6)\text{Rb}^-$ ,  $\text{Rb}(18\text{C}6)$ ,  $\text{Rb}^+(15\text{C}5)_2\text{Rb}^-$ ,  $\text{RbK}(18\text{C}6)$ , and  $\text{RbK}(15\text{C}5)_2\text{e}^-$  are mixtures that contain both the complexed rubidium cation and the rubidide anion. The EXAFS data for  $\text{Rb}^+(15\text{C}5)_2\text{e}^-$  and  $\text{Rb}^+(15\text{C}5)_2\text{Rb}^-$  indicate local structures around the rubidium cation similar to that of  $\text{Rb}^+(15\text{C}5)_2\text{Na}^-$ , a sodide whose crystal structure has been determined by X-ray diffraction. The radial distribution functions of the compounds  $\text{Rb}^+(18\text{C}6)\text{X}^-$  indicate different conformations of the 18-crown-6 ring in different salts.

A number of compounds that contain novel types of anionic species have been synthesized in our laboratory.<sup>1-4</sup> Alkalides

contain alkali metal anions, while electrides contain stoichiometrically trapped electrons as the anions. In both types of salts

<sup>†</sup> Michigan State University.

<sup>‡</sup> AT&T Bell Laboratories.

<sup>§</sup> Current address: Department of Chemistry, University of Illinois, Chicago, Chicago, IL 60680.

(1) Dye, J. L.; Ceraso, J. M.; Lok, M. T.; Barnett, B. L.; Tehan, F. J. *J. Am. Chem. Soc.* 1974, 96, 608-609.

(2) Dye, J. L. *Angew. Chem., Int. Ed. Engl.* 1979, 18, 587-598.